Analytical Models Correlation for Vehicle Dynamic Handling Properties

Daniel Vilela
danvil_br@hotmail.com
General Motors do Brasil Ltda.
Vehicle Synthesis
Analysis and Simulation Dept.
Sao Caetano do Sul
09550-051 SP, Brazil

Roberto Spinola Barbosa
roberto.barbosa@poli.usp.br
Escola Politécnica da Universidade de São Paulo
Departamento de Engenharia Mecânica
Sao Paulo
05508-900 SP, Brazil

Analytical models to evaluate vehicle dynamic handling properties are extremely interesting to the project engineer, as these can provide a deeper understanding of the underlying physical phenomena being studied. It brings more simplicity to the overall solution at the same time, making them very good choices for tasks involving large amounts of calculation iterations, like numerical optimization processes. This paper studies in detail the roll gradient, understeer gradient and steering sensitivity vehicle dynamics metrics, starting with analytical solutions available in the literature for these metrics and evaluating how the results from these simplified models compare against real vehicle measurements and more detailed multibody simulation models. Enhancements for these available analytical formulations are being proposed for the cases where the initial results do not present satisfactory correlation with measured values, obtaining improved analytical solutions capable of reproducing real vehicle results with good accuracy.
Keywords: *handling, vehicle dynamics, analytical solution, simulation*

Nomenclature

a_L	= lateral acceleration, m/s^2
b / c	= distance between CG and front/rear axle, m
F_{yf}, F_{yr}	= front and rear centrifugal force per axle, N
H_r	= effective roll arm, m
H_{CG}	= CG height to the ground, m
H_{rf}, H_{rr}, H_{rcg}	= vehicle roll center height at front axle, rear axle and CG position, m
K	= understeer gradient, rad/(m/s^2)
K_{bf}, K_{br}	= front and rear roll stiffness due to stabilizer bars, (Nm)/rad
K_{fyf}, K_{fyr}	= front and rear wheel steer angle stiffness with respect to tire lateral force, rad/N
K_{mzf}, K_{mzr}	= front and rear wheel steer angle stiffness with respect to tire align torque, rad/(Nm)
K_{roll}	= roll gradient, rad/(m/s^2)
K_s	= steering sensitivity, (m/s^2)/rad
K_{sf}, K_{sr}	= front and rear wheel roll stiffness due to springs, (Nm)/rad
K_T	= vehicle's total roll stiffness, (Nm)/rad
K_{tirf}, K_{tirr}	= front and rear wheel roll stiffness due to tires, (Nm)/rad
L	= wheelbase, m
M	= vehicle mass, Kg
$M_{ext,zf}$, $M_{ext,zr}$	= front and rear tire align torque, Nm
r_{dir}	= steering ratio, dimensionless
V_f, V_r	= front and rear tire velocity vector, m/s
T_{roll}	= roll moment, Nm

Greek Symbols

α_f, α_r	= front and rear tire slip angle, rad
δ	= front wheel steer angle, rad
θ	= vehicle roll angle, rad
$C_{\alpha f}$, $C_{\alpha r}$	= front and rear tire cornering stiffness, N/rad

Introduction

The most important vehicle dynamics steady state metrics, including roll gradient, understeer gradient and steering sensitivity, are covered in the traditional literature for vehicle dynamics, like Milliken (1995), Wong (2001) and Pacejka (2002). Each of these authors proposes analytical formulations to quantify these metrics, being these analytical solutions very important tools to the development engineer, who is able to have a very good understanding of the underlying phenomena and how the tuning variables affect each of these metrics. Besides that, the analytical solutions are extremely efficient in terms of computation time, allowing their usage for quick studies and very early assessments, as well as their linkage to numerical optimisation processes that take the advantage of their computational efficiency. Although these authors present simple analytical solutions to the metrics mentioned, none of them goes to the point of effectively comparing the results of their proposed analytical equations against real measurements to verify the accuracy of these formulations. Although the literature on the topic already presents analytical formulations for many of the usual vehicle dynamics metrics, few has been done in order to quantify the accuracy of these analytical models against real vehicle measurements and to understand the level of detail necessary to adequately capture the quantities of interest with such models.

On the other extreme, there are papers in the literature that present the comparison of physical measurements with the results of much more complex multibody models for non-linear dynamic manoeuvres, making usage of commercial multibody software packages, as it has been done using ADAMS® in previous works by Vilela (2001) and Prado et al. (2001). Rill (2006) and Adamski et al. (1999) describe in more details how some of these more complex multibody models work, showing the benefits of the flexibility that these models allow to the design engineer. By adopting these more complex models the engineer can get very accurate results for the vehicle dynamics response, including the steady-state metrics previously mentioned. The main drawback of this approach is that the more the multibody model gets details in the vehicle construction representation (a common multibody model easily contains more than 100 degrees of freedom – see example in Fig. 1), the more difficult and less intuitive is for the engineer the understanding of the basic dynamic phenomena being studied. Besides that, as these models usually contain lots of details in their construction, it is more difficult for the engineer to correctly guess which of the tuning variables affects more the metric of interest. Finally, the computational running time of such models is not as efficient as an analytical solution and, while this might not be a big problem for the normal development cycle in the industry with the current computing capabilities available, it might become a bottleneck for numerical optimisation procedures that demand a very high number of iterations to get to an optimum design. In a similar way, the application of active control systems for innovative active suspensions demands simpler models for its implementation, as presented by Shirahatt et al. (2008), where genetic algorithm optimization techniques and LQR control systems are applied to a model with 8 degrees of freedom.

Paper received 4 March 2010. Paper accepted 8 August 2011.
Technical Editor: Domingos Rade

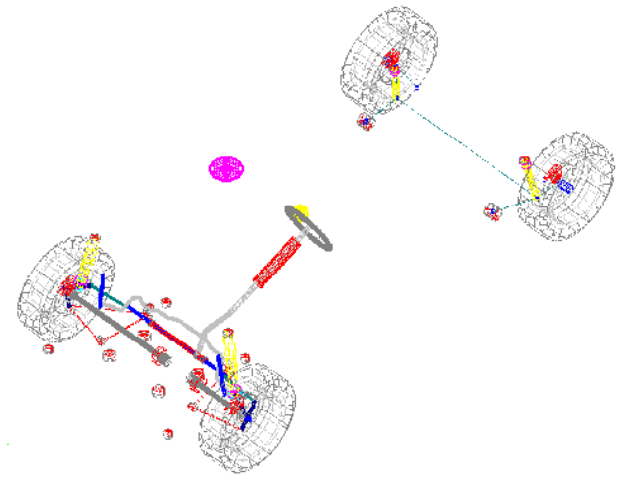

Figure 1. Graphical Representation of a Detailed Multibody Model (ADAMS®).

Following the idea that there is a need to understand better how these simple analytical formulations' results compare to real vehicle values and at which extent they can be applied for the vehicle development, the purpose of this paper is to present the analytical solutions available in the literature for roll gradient, understeer gradient and steering sensitivity metrics, comparing in the sequence the results from these simplified models against real vehicle measurements and more detailed multibody simulation models. In the cases where the initially calculated results do not present satisfactory correlation with measured values, enhancements for these analytical formulations are proposed, being the ultimate goal of this work to achieve/propose analytical solutions capable of reproducing real vehicle results with good enough accuracy that allow their usage for development purposes.

Roll Gradient Metric

The roll gradient is defined as the derivative of the vehicle body roll angle with respect to the lateral acceleration acting at its centre of gravity (CG), as indicated in Fig. 2. This value is usually evaluated in unities of degrees/g of lateral acceleration and can be physically measured through a constant radius circular manoeuvre with slow increase of the longitudinal velocity (and, therefore, the lateral acceleration), keeping as close as possible to a steady-state condition.

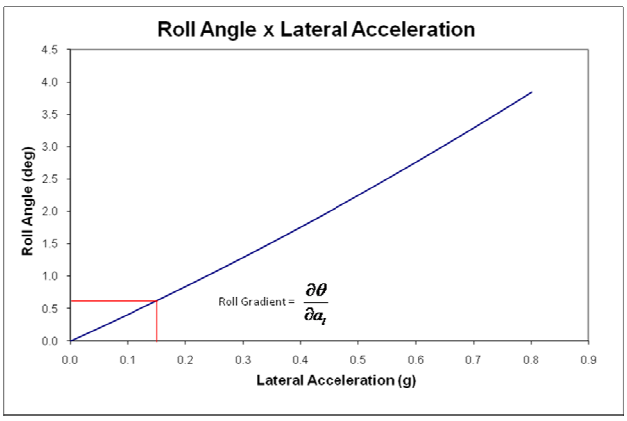

Figure 2. Definition of Roll Gradient.

Figure 3. Vehicle Rolling in a Curve.

This parameter quantifies in a very straightforward way how much a vehicle rolls during a curve manoeuvre, as illustrated in Fig. 3. In general, vehicles that roll less (i.e., present lower roll gradient values), are better evaluated in subjective terms by the drivers.

In order to analytically calculate the roll gradient, one has first to calculate the vehicle rolling stiffness K_T, in terms of torque per degree of body relative roll to the ground. The total rolling stiffness of the vehicle is calculated as the sum of the front and rear suspensions individual rolling stiffness and, in a first approach, this value can be calculated based only on the spring stiffness values, stabilizer bar stiffness values and tire radial stiffness values, as illustrated in Fig. 4.

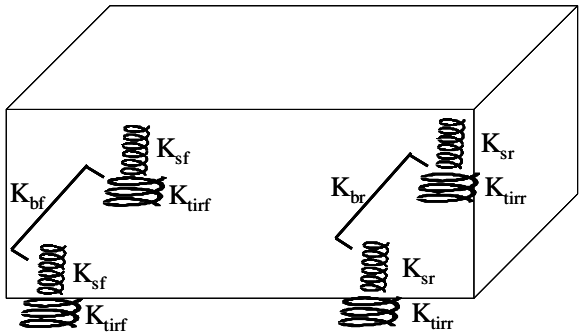

Figure 4. Main Elements for Roll Stiffness Calculation.

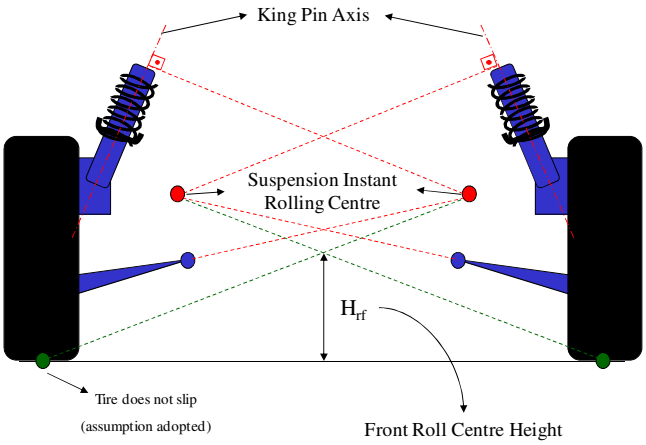

Figure 5. Front McPherson Suspension Roll Centre Height Calculation.

After this step, it is necessary to define the effective rolling arm H_r of the vehicle. Calculating the front and rear suspensions instant rolling centres, it is possible to join these points with the centre of the tire contact patch to the ground. Adopting the simplification that the tire contact patch to the ground does not move with respect to the local vehicle coordinates (i.e., there is no slip in the tires), the distance to the ground of the point in this line that crosses the centre plane of the vehicle is the front or rear suspension roll centre height. Figure 5 illustrates the calculation of the roll centre height for a McPherson front suspension type.

Following the same process for the front and rear suspensions, it is then possible to have a roll axis line in the vehicle's side view, and the distance between this line and the vehicle's CG is then defined as the effective rolling arm H_r, as illustrated in Fig. 6.

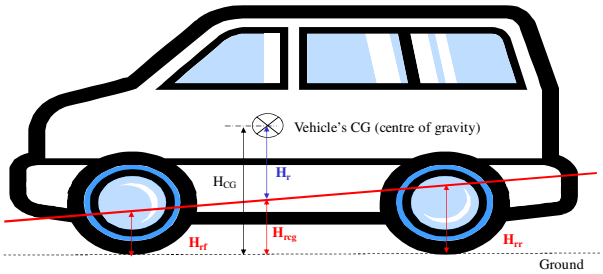

Figure 6. Vehicle's Roll Axis and Effective Rolling Arm.

With the effective rolling arm H_r defined, it is possible to calculate the roll moment T_{roll} applied to the vehicle due to the lateral acceleration imposed:

$$T_{roll} = M\, a_L H_r \tag{1}$$

The roll gradient K_{roll} is then calculated by the reaction between the roll moment T_{roll} and the vehicle's total roll stiffness K_T, as follows:

$$K_{roll} = \frac{T_{roll}}{\mathrm{K_T}} \tag{2}$$

Finally, using K_T in units of Nm/deg and normalizing the results for 1g of lateral acceleration in order to have the roll gradient results in the usual deg/g unit:

$$K_{roll} = \frac{\partial\theta}{\partial \mathrm{a_L}} = \frac{M\, g\, H_r}{K_T} \tag{3}$$

In order to understand the accuracy of the results from Eq. (3), these have been compared against physical measurements and a detailed multibody model (Fig. 1) for two different vehicles, here named vehicle 1 and vehicle 2. The physical measurements have been repeated in order to observe measurement variability and average results were considered for the comparison purposes. Data was acquired for the steering wheel angle, longitudinal velocity, lateral acceleration (accelerometers at vehicle's CG position) and roll angle with respect to the ground. The manoeuvre performed for the data acquisition was a slowly increasing longitudinal velocity over a constant radius in order to keep as close as possible to a steady-state condition. Figure 7 illustrates the test condition.

Figure 7. Vehicle Physical Test Condition.

The multibody model was simulated using the software ADAMS® and considering a fairly detailed description of the vehicle. The main characteristics of this detailed multibody model (depicted in Fig. 1) are:

- 256 degrees of freedom;
- Separate subsystem description for front suspension, rear suspension, steering system, front stabilizer bar, tires, body, powertrain and brakes;
- All masses, rotational inertia and joints between parts detailed;
- Non-linear representation of springs, shock absorbers and jounce bumpers;
- All suspension and steering compliant bushings represented by their non-linear stiffness characterization in all directions;
- Tires modelled with Magic Formula 5.2;
- Rear axle modelled as flexible body (finite element representation) and other bodies considered rigid.

The results are summarized in Table 1, demonstrating that the analytical model for the roll gradient metric herein presented provides good results compared to the physical measurements, and also in a similar level of accuracy compared to the detailed multibody model.

Table 1. Roll Gradient Results Comparison.

	K_{roll} (deg/g)	
	Vehicle 1	Vehicle 2
Experimental Measurements	4.93	6.62
Analytical Model Results	4.56	6.67
Detailed Multibody Model Results	4.59	5.99

Understeer Gradient Metric

The understeer gradient is defined as the derivative of the front tires average steer angle with respect to the lateral acceleration imposed to the vehicle at its centre of gravity, as indicated in Fig. 8. This value is usually evaluated in unities of degrees/g of lateral acceleration and, similarly to the roll gradient, can be physically measured through a constant radius circular manoeuvre with slow

increase of the longitudinal velocity (and, therefore, the lateral acceleration), keeping as close as possible to a steady-state condition.

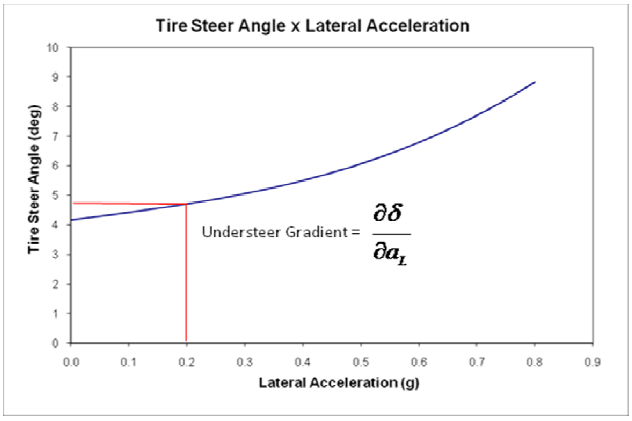

Figure 8. Understeer Gradient Definition.

This parameter evaluates the tendency of the vehicle, when in a steady-state curve manoeuvre, to be understeer (vehicle demands higher steering angles to keep the same curve radius at higher speeds) or oversteer (vehicle demands lower steering angles to keep the same curve radius at higher speeds). The vehicle is said to be neutral when the steering angle to keep a curve trajectory is dependant only on the curve radius and not on the vehicle speed. This definition is illustrated in Fig. 9.

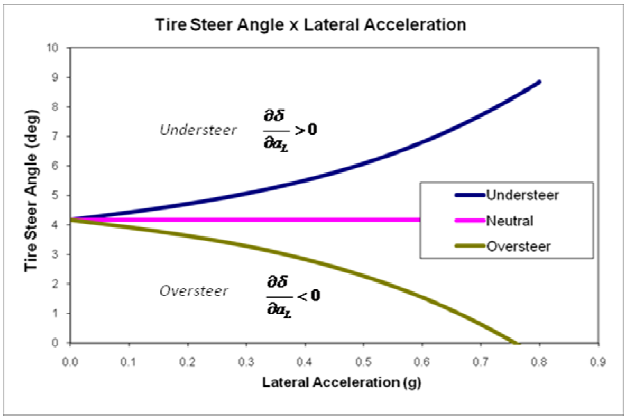

Figure 9. Understeer and Oversteer Definition.

A widely adopted simplified model to represent the vehicle for lateral dynamics is the bicycle model, where both right hand and left hand tires are grouped in a single entity and the vehicle is assumed to have its mass distributed along its centre line. This model is represented in Fig. 10 for a steady-state curve manoeuvre.

The centrifugal forces per axle can be calculated as follows:

$$F_{yf} = \frac{c}{L} M\, a_L \tag{4}$$

$$F_{yr} = \frac{b}{L} M\, a_L \tag{5}$$

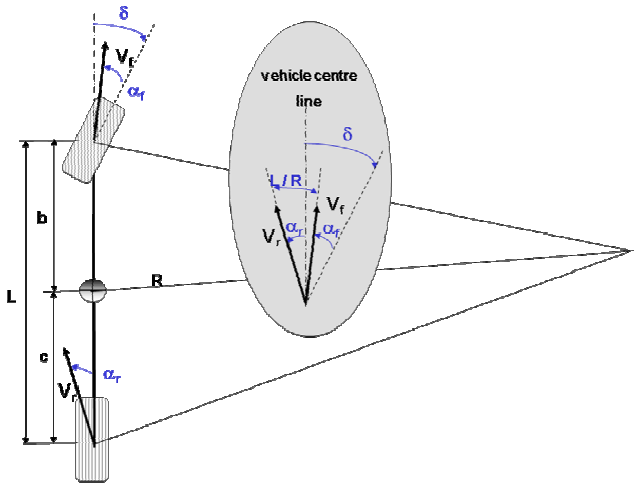

Figure 10. Bicycle Model for Steady-State Curve Manoeuvre.

Considering that the only external forces applied to the model are generated by the tire, and the tire forces can be calculated by a linear relationship between the slip angle and its cornering stiffness C_α, the following relationships are achieved (remembering there are 2 tires per axle in the bicycle model adopted):

$$F_{ext,yf} = 2C_{\alpha f}\alpha_f \tag{6}$$

$$F_{ext,yr} = 2C_{\alpha r}\alpha_r \tag{7}$$

Grouping Eqs. (4) to (7):

$$\alpha_f = \frac{F_{yf}}{2C_{\alpha f}} = \frac{M\, c\, a_L}{2LC_{\alpha f}} \tag{8}$$

$$\alpha_r = \frac{F_{yr}}{2C_{\alpha r}} = \frac{M\, b\, a_L}{2LC_{\alpha r}} \tag{9}$$

Finally, using the relationships shown in Fig. 9, the understeer gradient K can be calculated, as follows:

$$\delta = \frac{L}{R} + \left(\frac{c}{C_{\alpha f}} - \frac{b}{C_{\alpha r}}\right)\frac{M}{2L} a_L \tag{10}$$

$$K = \frac{\partial \delta}{\partial a_L} = \left(\frac{c}{C_{\alpha f}} - \frac{b}{C_{\alpha r}}\right)\frac{M}{2L} \tag{11}$$

Similarly to the roll gradient results, the understeer gradient values obtained with the Eq. (9) have been compared against physical measurements and a detailed multibody model. The results are summarized in Table 2.

Table 2. Understeer Gradient Results Comparison.

	K (deg/g)	
	Vehicle 1	Vehicle 2
Experimental Measurements	3.85	4.03
Analytical Model Results	0.53	1.16
Detailed Multibody Model Results	3.54	3.63

As it can be seen in the results from Table 2, this initial analytical model for the understeer gradient does not provide accurate results when compared to the physical measurements and the detailed multibody models. This difference can be explained by the factors that are not considered in this initial analytical formulation that considers only mass and tire properties. In order to improve the accuracy of the analytical model, the proposal of this work is to exchange of the terms $C_{\alpha f}$ and $C_{\alpha r}$ by equivalent terms $C'_{\alpha f}$ and $C'_{\alpha r}$ in the formulation previously described, which will take into consideration the following effects:

Additional effect 1 (e1): tire self-align torque effect

The tire self-align torque comes from the fact that the resultant lateral force generated by the tire is not coincident with the tire geometric centre, but rather located in a different point in the longitudinal axis of the tire. This distance is known as pneumatic trail t, and effectively changes the distances b and c between the lateral force application points and the CG of the vehicle as follows:

$$b' = b + t_f \tag{12}$$

$$c' = c + t_r \tag{13}$$

Additional effect 2 (e2): lateral load transfer

The lateral load transfer is a dynamic effect of the vehicle body under lateral acceleration, where there is a vertical (normal) load shift from the inner wheels to the outer wheels of the vehicle that is linearly proportional to the lateral acceleration that the vehicle is subject to and also the roll center height of the front/rear suspensions – more details about roll center height definition are shown by Milliken (1995) in the chapter 17.

The effect in the equations herein developed is that the front and rear individual tire cornering stiffness values $C_{\alpha f}$ and $C_{\alpha r}$ are dependent on the tire normal load. In this case, when the equations developed consider that the total cornering stiffness per axle is equal to 2 times the individual tire cornering stiffness at static normal load, the correct consideration to take into account in the lateral load transfer effect is to sum the inner and outer tire cornering stiffness individually. This can be done by adopting the average of the inner and outer tire values for the $C_{\alpha f}$ and $C_{\alpha r}$, as follows:

$$C_{\alpha f,llt} = \frac{C_{\alpha f,inner} + C_{\alpha f,outer}}{2} \tag{14}$$

$$C_{\alpha r,llt} = \frac{C_{\alpha r,inner} + C_{\alpha r,outer}}{2} \tag{15}$$

In general, for low lateral acceleration values (that is the range of interest of this study), this effect is not as much important as the ones previously described in the appendix section.

Additional effect 3 (e3): vehicle's suspension and steering system compliances

The forces and moments generated by the tires cause deformations in the suspension and steering systems of the vehicle, as illustrated in Fig. 11.

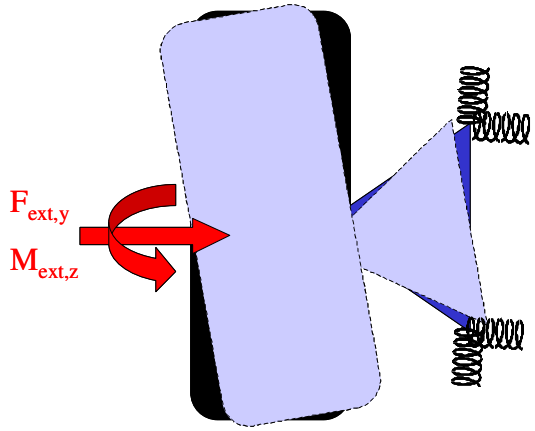

Figure 11. Effect of Vehicle's Suspension and Steering System Compliances.

Assuming that there is a linear relationship between the tire lateral force and align torque with the angle generated in the front/rear wheels due to the suspension and steering system compliance, the front/rear slip angles can be redefined as:

$$\alpha'_f = \alpha_f - F_{ext,yf}\, K_{fyf} - M_{ext,zf}\, K_{mzf} \tag{16}$$

$$\alpha'_r = \alpha_r - F_{ext,yr}\, K_{fyr} - M_{ext,zr}\, K_{mzr} \tag{17}$$

Same as the lateral force, the front/rear tire align torque is also assumed to be linear with respect to the tire slip angle as follows:

$$M_{ext,zf} = 2\, C_{mz\alpha f}\, \alpha_f \tag{18}$$

$$M_{ext,zr} = 2\, C_{mz\alpha r}\, \alpha_r \tag{19}$$

It is possible to define then new auxiliary terms B_f and B_r:

$$B_f = 1 + 2C_{\alpha f}\, K_{fyf} + 2C_{mz\alpha f}\, K_{mzf} \tag{20}$$

$$B_r = 1 + 2C_{\alpha r}\, K_{fyr} + 2C_{mz\alpha r}\, K_{mzr} \tag{21}$$

And the slip angles adjusted by the suspension and steering system compliances can be then defined as:

$$B_f\, \alpha'_f = \alpha_f \tag{22}$$

$$B_r\, \alpha'_r = \alpha_r \tag{23}$$

Additional effect 4 (e4): kinematic steering variation with vertical suspension travel

The wheels also steer due to the vertical travel of the suspension, being this variation a function of the vehicle's specific suspension/steering geometry. This effect is shown in more detail by Milliken (1995) in the chapter 19 and is also known in the literature as roll steer.

Considering that the vehicle is on a plane road, the vertical travel of the suspension is only a function of the vehicle roll angle θ, and the later can be considered linearly related to the lateral acceleration through the roll stiffness of the vehicle in the range of interest for this work (less than 0.4 g's of lateral acceleration). In this sense, following the same rationale previously described for the suspension and steering compliances, the kinematic steering variation with vertical suspension travel can be described through auxiliary terms $B_{f,rs}$ and $B_{r,rs}$, where the index **rs** refers to the roll steer effect. It is also interesting to mention that, in most cases, the front steered suspension is more sensitive to this effect than the rear suspension.

Summation of additional effects

The consideration of the effects previously described for the tire self-align torque, vehicle's suspension and steering system compliances, kinematic steering variation with vertical suspension travel and lateral load transfer can be implemented in the analytical solution through the substitution of the terms $C_{\alpha f}$ and $C_{\alpha r}$ by the equivalent terms $C'_{\alpha f}$ and $C'_{\alpha r}$ in the formulation previously described, as follows:

$$C'_{\alpha f} = \frac{C_{\alpha f,llt}\, c}{B_f\, B_{f,rs}\, c'} \tag{24}$$

$$C'_{\alpha r} = \frac{C_{\alpha r,llt}\, b}{B_r\, B_{r,rs}\, b'} \tag{25}$$

The results of adding each of the previously described effects (e1, e2, e3 and e4) are summarized in Table 3. A graphical representation intended to help the visualization of the individual contributions is shown in Figs. 12 and 13.

Table 3. Understeer Gradient Results Comparison – Additional Effects.

		K (deg/g)	
		Vehicle 1	Vehicle 2
	Experimental Measurements	3.85	4.03
Base Model	Initial Analytical Model Results	0.53	1.16
e1	e0 + Tire Self-Align Torque	0.66	1.37
e2	e1 + Lateral Load Transfer	0.76	1.49
e3	e2 + Vehicle's Suspension and Steering System Compliances	2.71	3.73
e4	e3 + Kinematic Steering Variation with Vertical Suspension Travel	3.92	4.04
Multibody	Detailed Multibody Model Results	3.54	3.63

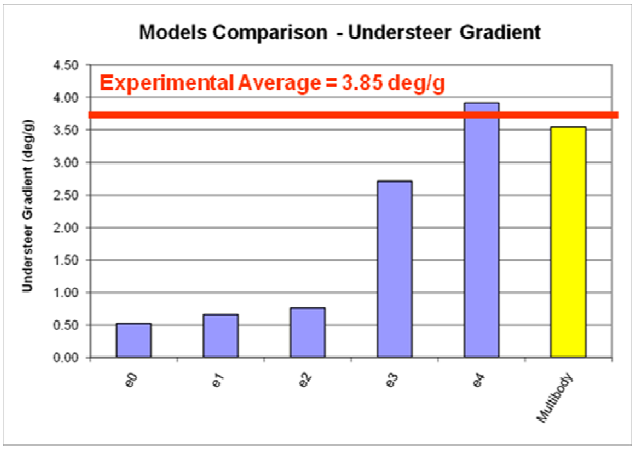

Figure 12. Vehicle 1 Understeer Gradient Results Comparison – Additional Effects.

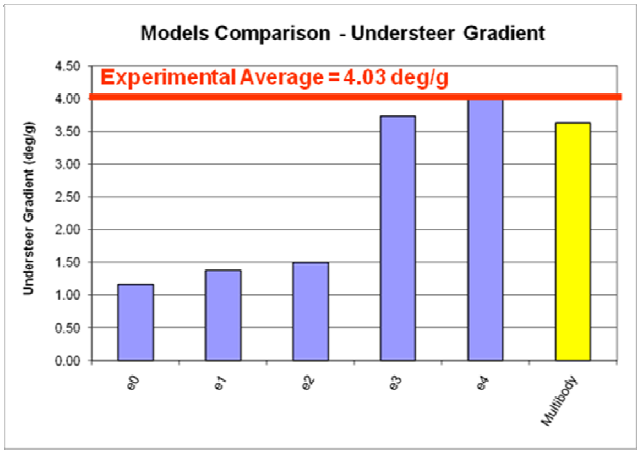

Figure 13. Vehicle 2 Understeer Gradient Results Comparison – Additional Effects.

Steering Sensitivity Metric

The steering sensitivity is defined as the derivative of the lateral acceleration with respect to the steering wheel angle imposed to the vehicle at its centre of gravity, as indicated in Fig. 14. This value is usually evaluated in unities of g/100 degrees of steering wheel angle (SWA) – the multiplication of the unit by a 100 times factor is intended to get numerical values in the range of 1.0, making them easier to work with. Analogous to the previous metric, the steering sensitivity can be physically measured through a constant radius circular manoeuvre with slow increase of the longitudinal velocity (and, therefore, the lateral acceleration), keeping as close as possible to a steady-state condition.

This parameter evaluates the responsiveness of the vehicle with respect to the driver inputs at the steering wheel, where low values can bring a subjective feeling of a slow response or lack of response from the vehicle and, at the same time, values too high are associated with the subjective feeling of a very fast response more difficult to control, as small disturbances in the steering wheel already produce a reasonable amount of lateral acceleration, changing its trajectory. The steering sensitivity is closely related to the understeer gradient, being inversely proportional to that one and to the overall steering ratio of the vehicle. Some of the reasons that make it important to consider this metric independently of the

understeer gradient are that many projects are limited to use the same steering system for a wide range of vehicles, making the compromise between understeer gradient and steering sensitivity more difficult to be achieved. Besides that, as the steering sensitivity is inversely proportional to the overall steering ratio of the vehicle, there is also a compromise between this metric and the steering effort of the vehicle, what is especially critical for non-assisted (manual) steering systems.

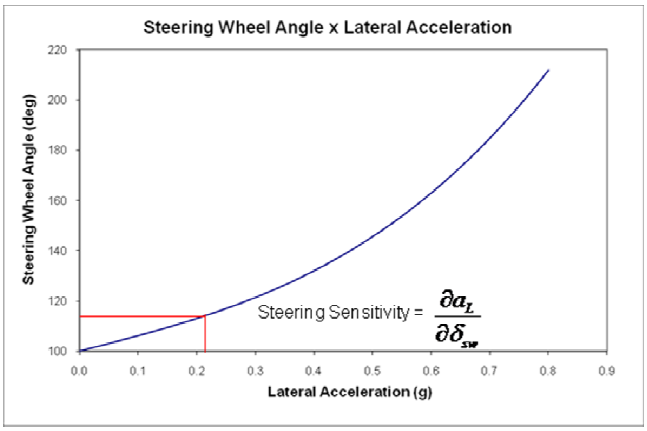

Figure 14. Steering Sensitivity Definition.

The steering sensitivity K_s is defined by the Eq. (27), where K is the understeer gradient as previously defined and r_{dir} is the on-center overall steering ratio, i.e. the ratio between steering wheel angle and average front wheels steer angle, which can be described by the derivative of the relationship between both values, as indicated in Eq. (26).

$$r_{dir} = \frac{\partial \delta_{vol}}{\partial \delta} \tag{26}$$

$$K_s = \frac{\partial a_L}{\partial \delta_{vol}} = \frac{\partial a_L}{\partial \delta}\frac{\partial \delta}{\partial \delta_{vol}} = \frac{1}{\mathrm{K}}\frac{1}{r_{dir}} \tag{27}$$

Table 4. Steering Sensitivity Results Comparison.

		Steering Sensitivity (g/100° SWA)	
		Vehicle 1	Vehicle 2
	Experimental Measurements	1.55	1.59
Base Model	Initial Analytical Model Results	11.17	5.49
e1	e0 + Tire Self-Align Torque	8.95	4.63
e2	e1 + Lateral Load Transfer	7.75	4.26
e3	e2 + Vehicle's Suspension and Steering System Compliances	2.17	1.71
e4	e3 + Kinematic Steering Variation with Vertical Suspension Travel	1.50	1.58
Multibody	Detailed Multibody Model Results	1.66	1.76

In a similar way to what has been done in the case of the understeer gradient, the steering sensitivity analytical model has been improved by the inclusion of additional effects, and the experimental results and comparison between the analytical models for each improvement step are shown in Table 4. A graphical representation intended to help the visualization of the individual contributions is shown in Figs. 15 and 16.

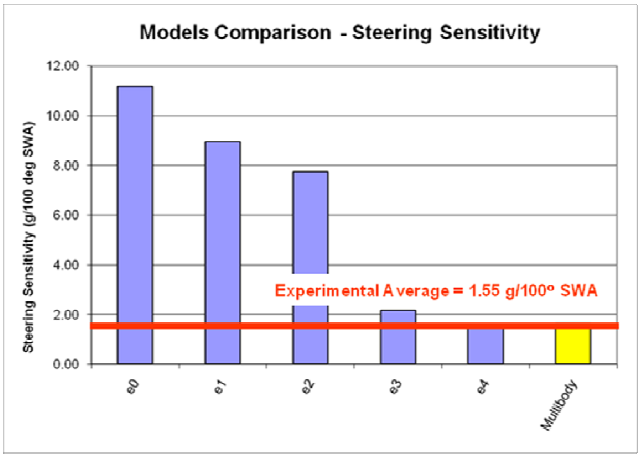

Figure 15. Vehicle 1 Steering Sensitivity Results Comparison.

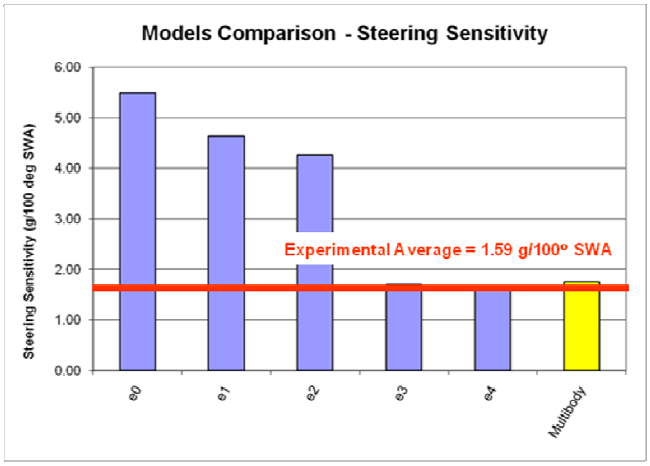

Figure 16. Vehicle 2 Steering Sensitivity Results Comparison.

Conclusions

This paper has described the analytical model for the roll gradient, understeer gradient and steering sensitivity metrics. The results of each of these analytical solutions have been compared against physical measurements and more detailed multibody models.

The comparison has shown that the analytical solutions presented in the commonly known literature (Milliken, 1995; Wong, 2001 and Pacejka, 2002) are accurate enough to represent the roll gradient, but the initial results for the understeer gradient and steering sensitivity are not enough accurate. The paper has then described the inclusion of additional effects in these analytical formulations that affect the phenomena related to these metrics: namely steer compliance and steer angle variation due to suspension vertical travelling. The comparative results against the

physical measurements indicate that these additional effects are indeed very important to adequately represent these metrics, and the accuracy improvements obtained for each additional effect have been presented. This make possible for the engineer or analyst to have a quantitative idea of the importance of each of these additional effects.

The results of the final analytical models achieved are considered to have enough accuracy to allow their usage for development purposes. The fact that these analytical models are much more efficient in terms of computational time compared to the more detailed multibody models makes them excellent options to be used with numerical optimization routines. These advantages are especially interesting in the early development phases of a new project. Additionally, the analytical models can give much more insight of the underlying phenomena to the engineer compared to the more detailed models, letting it very clear how the tuning variables affect each of these metrics.

Finally, future developments of this work might include additional metrics and their validation against physical measurements following the same process, making it possible the extension of the analytical modelling usage for vehicle dynamics characterization.

References

Adamski, D., Schuster, C., Hiller, M., 1999, "Advances in Modelling of Mechatronic Systems: The Toolset FASIM_C++ for the Simulation of Vehicle Dynamics", *Journal of the Brazilian Society of Mechanical Sciences and Engineering*, Vol. 21, No. 4.

Milliken, W.F., Milliken, D.L., 1995, "Race Car Vehicle Dynamics", SAE, Warrendale, USA.

Pacejka, H.B., 2002, "Tire and Vehicle Dynamics", SAE, Warrendale, USA.

Prado, M., Cunha, R.H., Costa Neto, A., Costa, A., Mancosu, F., Savi C., Délboux, J.E., 2001, "Bus Handling Analysis and Experimental Validation Using the Multibody System Technique", In: SAE Brazil 2001 Congress and Exhibit, 2001, São Paulo, SP, SAE Paper 2001-01-3966.

Rill, G., 2006, "Vehicle Modeling by Subsystems", *Journal of the Brazilian Society of Mechanical Sciences and Engineering*, Vol. 28, No. 4.

Shirahatt, A., Prasad, P.S.S., Panzade, P., Kulkarni, M.M., 2008, "Optimal Design of Passenger Car Suspension for Ride and Road Holding". *Journal of the Brazilian Society of Mechanical Sciences and Engineering*, Vol. 30, No. 1.

Vilela, D., 2001, "Vehicle Dynamics Simulation Correlation with Field Maneuvers", In: SAE Brazil 2001 Congress and Exhibit, 2001, São Paulo, SP, SAE Paper 2001-01-3799.

Wong, J.Y., 2001, "Theory of Ground Vehicles", John Wiley & Sons Inc., New York, USA.